

## Localized States at the Conduction-Band Edge of Amorphous Silicon Nitride Detected by Resonance Photoemission

L. Ley,<sup>(a)</sup> R. Kärcher, and R. L. Johnson

Max-Planck Institut für Festkörperforschung, D-7000 Stuttgart 80, Federal Republic of Germany

(Received 23 April 1984)

The Si  $L_{II,III}$  absorption edge in amorphous silicon nitride ( $a\text{-SiN}_x\text{:H}$ ) exhibits a Fano-type antiresonance just below threshold for  $x=1.20$  and  $1.40$ . At the same energy the valence-band photoemission cross section is resonantly enhanced in these samples for those features that carry an appreciable Si-3s-derived partial density of states. We argue that the Fano resonance involves Si-Si antibonding states at the bottom of the conduction bands that become localized as their number decreases with increasing nitrogen content compared to that of Si-N bonds.

PACS numbers: 71.55.Jv, 78.70.Dm, 79.60.Eq

We have studied the Si  $2p$  ( $L_{II,III}$ ) absorption edge in a series of amorphous hydrogenated silicon nitride compounds ( $a\text{-SiN}_x\text{:H}$ ) with varying nitrogen content  $x$ . In a narrow range of nitrogen concentration around  $x=1.33$  which corresponds to stoichiometric  $\text{Si}_3\text{N}_4$ , a dip in the absorption spectrum is observed just below the  $L_{II,III}$  (see Fig. 1.) This dip can be described as a Fano antiresonance in the absorption cross section. Such a description is supported by a similar resonance in the partial photoelectric cross section (PPCS) of certain features in the valence band at the same photon energy.

Fano resonances are multielectron effects.<sup>1</sup> They occur when excited bound states of an  $N$ -electron system lie above the ionization threshold of the system. The bound state can then mix via configuration interaction with states formed by coupling a continuum function to an  $(N-1)$ -electron ion core. The resulting eigenstate, when reached by resonant photoexcitation, has a certain probability to autoionize into the different  $(N-1)$ -electron states, each of which is identified by the kinetic energy of the outgoing electron. This direct recombination of the discrete excitation interferes with the ordinary photoionization process taking place at the same energy and leads thus to the characteristic, resonantlike modification of the total and partial photoexcitation cross sections. Configuration interaction as a way to take correlation into account is maximized when the discrete excitation is highly localized. It is therefore not surprising that strong Fano resonances in solids are mainly observed near core-level excitations involving  $4f$  valence electrons.<sup>2</sup> In semiconductors the necessary localization is provided primarily by core surface excitons.<sup>3</sup> A small PPCS resonance has been reported at the core conduction-band exciton in silicon<sup>4</sup> but this interpretation of the data has been challenged.<sup>5</sup> On

the basis of the results of Fig. 1 and the analysis presented below we suggest that an alternative localization mechanism may be operative in  $a\text{-SiN}_x\text{:H}$  that is characteristic for amorphous systems: states at the conduction-band edge converted from bandlike and extended to defectlike and localized as the composition of the material changes.

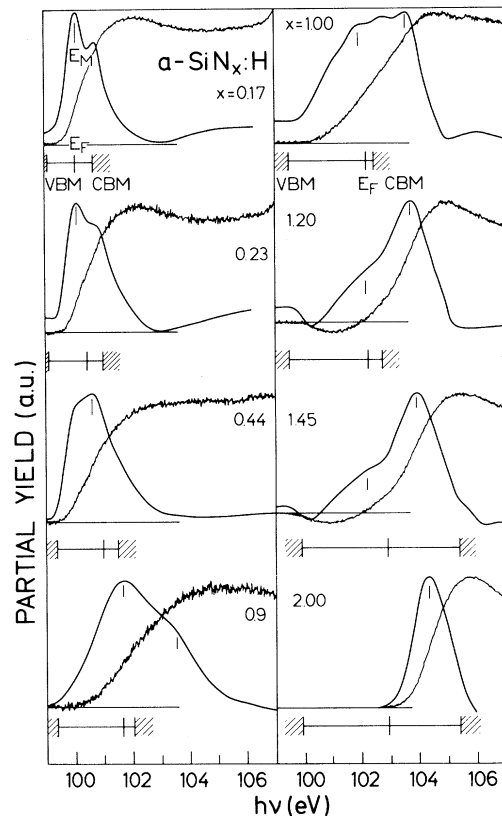


FIG. 1. Partial yield spectra of  $a\text{-SiN}_x\text{:H}$  and their first derivatives in the neighborhood of the Si  $2p$  threshold. The slowly varying photoelectric yield due to  $\text{VB} \rightarrow \text{CB}$  transitions has been subtracted.

The samples used in our study were prepared as thin films by the glow-discharge decomposition of  $\text{SiH}_4\text{-N}_2$  mixtures.<sup>6</sup> These films contain between 25 and 35 at.% hydrogen. The nitrogen content was determined with an accuracy of 10% from the intensities of the N 1s and Si 2p core lines as measured by x-ray-induced photoemission (XPS) and calibrated against a stoichiometric  $\text{Si}_3\text{N}_4$  sample. Synchrotron radiation from the DORIS storage ring in Hamburg in conjunction with a plane-grating monochromator was used to measure the partial photoelectron yield and photoelectron energy distribution curves (EDC's) in the photon-energy range corresponding to the Si  $L_{\text{II,III}}$  edge. The resolution of the yield measurements, which are equivalent to optical absorption measurements, was 0.1 eV and the EDC's were recorded with a resolution of 0.3 eV.

Figure 1 shows the yield spectra of a series of  $a\text{-SiN}_x\text{:H}$  films for  $x$  between 0.17 and 2.0.<sup>7</sup> The  $L_{\text{II,III}}$  edge is superimposed on a structureless continuum of comparable strength that is suppressed in the spectra of Fig. 1. The continuum corresponds to transitions from the valence bands to states high in the conduction bands ( $\text{VB} \rightarrow \epsilon l$ ). For  $x = 1.20$  and 1.45 we observe a dip just before the yield starts to rise. We attribute this window of transparency to the Fano interference between the continuum of  $\text{VB} \rightarrow \epsilon l$  transitions and excitations from the Si 2p core states to localized states at the bottom of the conduction bands. The resonant enhancement of the cross section that is expected to follow the dip on the basis of Fano's theory is not easily distinguished in the spectra of Fig. 1, because it merges into the steep rise due to noninterfering transitions into the continuum of delocalized conduction states.

The resonant enhancement is in principle readily observed if we follow the PPCS of the  $\text{VB} \rightarrow \epsilon l$  transitions as a function of photon energy. This is accomplished in constant-initial-state spectroscopy (CIS) whereby photon and electron energies are scanned in parallel so that only transitions with a fixed initial-state energy contribute to the photoelectron current. The variation in photoelectric cross section of selected features in the valence bands of  $a\text{-SiN}_{1.2}\text{:H}$  so obtained are shown in Fig. 2. Peaks C and D exhibit a pronounced resonant enhancement of their cross section around  $h\nu = 100$  eV, which amounts to about 10% of the non-resonant "background" absorption. The resonance of peak D interferes with the Si  $L_{\text{VV}}$  Auger emission as described in Ref. 5. The Auger contribution (see Fig. 3) was estimated by use of the Auger line

shape as measured in EDC's taken at higher photon energies. The line shapes of these resonances are well described by the Fano profile  $I(\epsilon) = (q + \epsilon)^2 / (1 + \epsilon^2)$  with a reduced energy scale  $\epsilon = (E - E_0) / \Gamma$ .  $\Gamma$  and  $E_0$  refer to the width and energy of the resonance, respectively. The much weaker resonances of peaks A and B are typical for the enhancement seen throughout the valence bands in samples with  $x$  values other than 1.20 or 1.45.

Figure 3 shows the results of least-squares fits of the absorption edge and the photoemission resonances of peaks C and D of the  $a\text{-SiN}_{1.2}\text{:H}$  EDC's to the Fano profile. The fit of resonance D is based on data points below  $E_0$ , i.e., in a region where the shape of the resonance is least susceptible to the assumptions made in correcting for the  $L_{\text{VV}}$  contribution. The lines represent the superposition of two Fano resonances corresponding to transitions

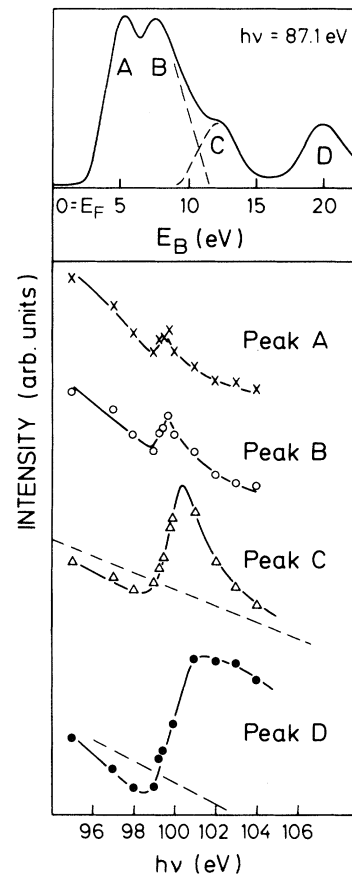


FIG. 2. (Top panel) The valence-band EDC of  $a\text{-SiN}_{1.2}\text{:H}$  and (lower panel) the constant-initial-state spectra of peaks A through D in the neighborhood of the Si 2p threshold.

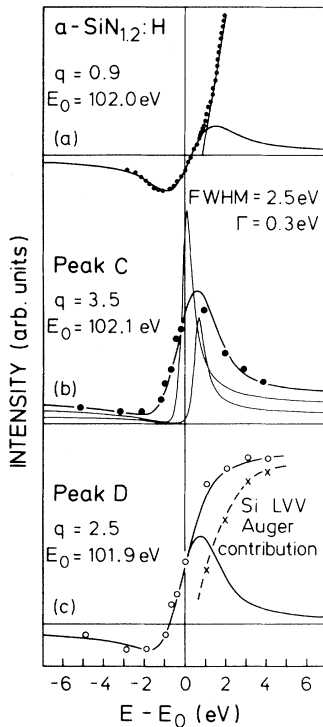


FIG. 3. Fano-line-shape fits to the Si  $2p$  threshold and the resonant, photoemission cross sections of peaks C and D. A linear nonresonant background as indicated by the dashed lines in Fig. 2 has been subtracted prior to fitting. The unbroadened spin-orbit components are shown for peak C only.

from the  $2p_{1/2}$ ,  $2p_{3/2}$  ( $L_{II}$ ,  $L_{III}$ ) spin-orbit doublet. A 0.6-eV spin-orbit splitting and the statistical ratio of 1:2 were measured. It was further necessary to allow for a Gaussian broadening of the resonances and we required that the Gaussian width (full width at half maximum) and the parameter  $\Gamma$  remain unchanged for all three resonances. The resulting fit parameters are listed next to each line in Fig. 3. A resonance energy  $E_0$  of  $102.0 \pm 0.1$  eV is obtained consistently for all three profiles.

We have analyzed the shape of the Si  $2p$  absorption edge in terms of its first derivative (compare Fig. 1) and we take the maximum of the derivative,  $E_M$ , as a measure of the edge position. Also included in Fig. 1 are the positions of the valence-band maximum (VBM), the Fermi level ( $E_F$ ), and the conduction-band minimum (CBM) that were obtained by combining core and VB EDC's<sup>6</sup> with optical absorption spectra from Ref. 8. It is evident that the  $L_{II,III}$  edge is lowered by excitonic effects. The excitonic binding energies,  $E_x = \text{CBM} - E_M$ , reach values ( $E_x = 1.3$  eV for  $x = 0.44$  and 1.0) that are substantially larger than those quoted<sup>9</sup> for  $c$ -Si or

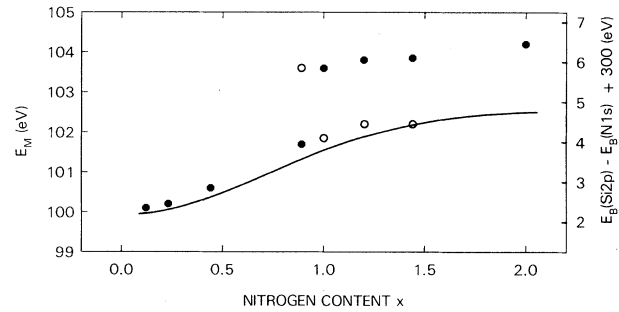


FIG. 4. The position of structure  $E_M$  as indicated in the derivative of the yield spectra in Fig. 1 plotted vs the nitrogen content  $x$ . Full circles refer to maxima and open circles to shoulders. Also shown as a solid line are the Si  $2p$  binding energies referenced to those of the unshifted N  $1s$  line.

$a$ -Si as a result of the reduced screening provided by silicon nitride with its lower dielectric constant. It is equally apparent that no particularly large  $E_x$  is found for  $x = 1.20$  ( $E_x = 0.6$  eV) or  $x = 1.45$  ( $E_x = 1.5$  eV), a fact which excludes excitonic localization as the major reason for the observed Fano resonance.

For a sharp (compared to the natural width of the core levels) conduction-band edge the first derivative reflects the spectral distribution of the initial states. This is seen to be the case for the  $a$ -SiN<sub>0.17</sub>:H sample, where the double structure reproduces the intensity ratio and the spin-orbit splitting of the Si  $2p_{1/2,3/2}$  core levels. With increasing nitrogen content, the edge broadens and a second threshold appears as witnessed by the shoulder in the derivative for  $x = 0.90$ . This shoulder develops eventually into the main transition accompanied by a renewed sharpening of the edge. In Fig. 4, we have plotted the position of the two transitions (their  $E_M$  values) as a function of  $x$ . Also shown in Fig. 4 is the binding energy of the Si  $2p$  core level,  $E_b(\text{Si } 2p)$ , as measured in XPS relative to that of the N  $1s$  line which shows negligible chemical shift.<sup>6</sup> The 2.7-eV chemical shift in  $E_b(\text{Si } 2p)$  is due to the successive replacement of Si-Si bonds by the more electronegative Si-N bonds.<sup>6</sup> It is apparent that the increase in the absorption threshold can be accounted for by the chemical shift of the initial state alone and the same holds qualitatively for the broadening of the edge as well. The edge position extrapolates to that of  $a$ -Si:H for  $x = 0$  and it is thus reasonable to assume that we are dealing with transitions from Si  $2p$  core to Si-Si antibonding states which determine the bottom of the conduction band up to  $x = 1.45$ . Beginning at  $x \approx 0.9$  transitions to Si-N antibonding states start to con-

tribute noticeably to the spectrum and give rise to the shoulder 1.8 eV above the main peak in the derivative. These transitions dominate above  $x = 1.0$  where according to our previous study  $\sim 68\%$  of all Si-Si bonds have been replaced by Si-N bonds.<sup>6</sup> The energy of the Si-N antibonding states is 1.8 eV higher than that of the Si-Si antibonding states and the transition energies are again seen to track those of the Si  $2p$  levels. In nearly stoichiometric samples ( $x \approx 1.3$ ), when most of the Si-Si bonds are replaced by Si-N bonds, the remaining Si-Si bonding and antibonding states localize because of a lack of neighbors with sufficient overlap to form bands in the presence of vertical and lateral disorder characteristic for an amorphous solid.<sup>10</sup> Transitions from Si  $2p$  core levels into these localized antibonding states are in our opinion responsible for the observed Fano resonances. The possibility of observing them is limited on the one hand by the requirement of localization which sets in for our samples between  $x = 0.90$  and  $x = 1.20$ . The requirement that they are present in sufficient numbers, on the other hand, prevents them from being observed in  $\text{SiN}_{2.0}\text{:H}$  specimens.

The Gaussian broadening of the Fano profiles reflects variations in the Si  $2p$  binding energies as well as a distribution of final-state energies. The number of Si-N bonds on a given Si atom determines the initial state energy via chemical shifts that amount to  $\sim 0.7$  eV per Si-N bond.<sup>6</sup> Differences in the chemical environment of the Si-Si bonds will similarly affect the energy of the Si-Si antibonding states.

The Si  $2p$  core absorption spectrum is governed by the dipole selection rule. Transitions from Si  $2p$  states lead therefore predominantly to antibonding states with Si  $3s, 3d$  character which we denote by  $\sigma^*(s, d)$ . The matrix element responsible for the Fano interaction is of the form  $\langle \sigma^*(s, d), \sigma(s) | V | 2p, \epsilon l \rangle$ . The discrete transition takes place between  $2p$  and  $\sigma^*(s, d)$  while the interfering continuum connects Si-Si bonding states denoted by  $\sigma$  with final states  $\epsilon l$ . The matrix element is maximized when the bonding states are also derived from Si  $3s$  orbitals. This is the case for peaks *C* and *D* of the valence bands which are the only ones with appreciable Si  $3s$  character<sup>5</sup> and it explains the lack of resonant enhancement in the remainder of the valence bands.

The degree of localization we are dealing with here exceeds most likely that necessary to affect

transport and establish a mobility edge in the tail states of most disordered semiconductors.<sup>10</sup> The results indicate, however, that under favorable conditions "chemically" induced localization may be detected spectroscopically.

We finally point out that the 1.8-eV difference in the position of the Si-Si and Si-N antibonding states accounts nicely for the 1.9-eV conduction-band discontinuity at the  $\text{Si:Si}_3\text{N}_4$  interface.<sup>11</sup> By the same token, the Si-Si antibonding defect states lie approximately 1.8 eV below the conduction-band minimum in the gap.

The support by the members of HASYLAB and helpful discussions with M. Cardona and J. Barth are gratefully acknowledged. One of us (L.L.) thanks the IBM Watson Research Center for its hospitality while this report was written. This work was in part supported by der Bundesminister für Forschung und Technologie.

---

(a) Present address: IBM T. J. Watson Research Center, Box 218, Yorktown Heights, N. Y. 10598

<sup>1</sup>U. Fano, Phys. Rev. **124**, 1866 (1961).

<sup>2</sup>See, e.g., F. Gerken, J. Barth, and C. Kunz, in *X-ray and Atomic Inner-shell Physics—1982*, edited by B. Crasemann, AIP Conference Proceedings No. 94 (American Institute of Physics, New York, 1982), p. 602.

<sup>3</sup>G. J. Lapeyere and J. Andersen, Phys. Rev. Lett. **35**, 117 (1975); F. Sethe, P. Perfetti, F. Patella, C. Quaresima, C. Capasso, M. Capozzi, and A. Savoia, Phys. Rev. B **28**, 4882 (1983).

<sup>4</sup>K. L. I. Kobayashi, H. Daimon, and Y. Murata, Phys. Rev. Lett. **50**, 1701 (1983).

<sup>5</sup>R. A. Riedel, M. Turowski, G. Margaritondo, and P. Perfetti, Phys. Rev. Lett. **52**, 1568 (1984).

<sup>6</sup>R. Kärcher, L. Ley, and R. L. Johnson, Phys. Rev. B (to be published).

<sup>7</sup>Samples with a nitrogen concentration higher than that corresponding to stoichiometric  $\text{Si}_3\text{N}_4$  ( $x = 1.33$ ) can be obtained because a sizable fraction of nitrogen atoms forms N-H bonds (see also Ref. 5).

<sup>8</sup>H. Kurata, M. Hirose, and Y. Osaka, Jap. J. Appl. Phys. **20** L811 (1981).

<sup>9</sup>L. Ley, in *Hydrogenated Amorphous Silicon II*, edited by J. Joannopoulos and G. Lucovsky (Springer-Verlag, Berlin, 1984), p. 61.

<sup>10</sup>N. F. Mott and E. A. Davis, *Electronic Processes in Non-Crystalline Semiconductors* (Clarendon, Oxford, 1979), p. 48.

<sup>11</sup>D. J. DiMaria and P. C. Arnett, Appl. Phys. Lett. **26**, 711 (1975).